Chapter 6
Radiometric Calibration

Abstract. The subject of this chapter is radiometric calibration. This is the conversion of the input image values to a common radiometric scale. The transformation to such a scale is of critical importance in image fusion. Without a common radiometric base it is not possible to fuse images which were acquired at different illuminations, or under different atmospheric conditions or captured by different sensors. Radiometric calibration is used in both image fusion and in feature map fusion. For the sake of concreteness, we shall concentrate on the radiometric calibration of two input images A and B.

6.1 Introduction

The transformation to a common radiometric base is known as radiometric calibration, or normalization, which may in turn be divided into two types: absolute and relative. The absolute radiometric correction converts the digital counts of a pixel in the input image to radiance values. The absolute radiometric correction tends to be more accurate than the relative correction, but it needs sensor parameters, atmospheric refraction parameters and other data that are difficult to obtain. The difficulty in obtaining the above accurate atmospheric and sensor parameters makes relative radiometric normalization an attractive alternative. In relative radiometric normalization we designate one image as a reference image and adjust the radiometric properties of the second, or floating, image to match the reference image. The normalized image should therefore appear to have been acquired under the same conditions as the reference image.

Example 6.1. Intensity Standardization in MR Images [12]. Brain MR images present significant variations across patients and scanners. Consequently, training a classifier on a set of images and subsequently using it for brain segmentation may yield poor results. Significantly better segmentation is obtained if the image intensities are standardized beforehand.

6.2 Histogram Matching

In this section we consider the radiometric calibration technique known as histogram matching. This is one of the simplest and effective unsupervised radiometric alignment techniques. It uses the equalization of the histogram of the image B to the histogram of the reference image A. The method is a statistical method and does not require the accurate spatial alignment of the two images. It is therefore useful for calibrating images of the same scene which are acquired on different dates or with different illumination or atmospheric effects.

The goal of histogram equalization is to transform the image B in such a way that its pdf matches the pdf of the reference image A. Suppose b denotes a given pixel feature whose probability density function (pdf) and cumulative distribution function (cdf) are, respectively, $p_B(b)$ and $c_B(b)$, where $c_B(b) = \int_{-\infty}^{b} p_B(b)db$. We seek a function $a = F(b)$ which maps $p_B(b)$ into the corresponding reference pdf, $p_A(a)$. This is obtained by equating $c_B(b)$ and $c_A(a)$, where $c_A(a) = \int_{-\infty}^{a} p_A(a)da$:

$$c_B(b) = c_A(a) = c_A(F(b)) \,,$$

or

$$a = F(b) = c_A^{-1}(c_B(b)) \,,$$

where c_A^{-1} denotes the inverse of c_A [1].

If the pixel gray-levels in B are distinct, then histogram matching B to A is straightforward as the following example shows.

Example 6.2. Histogram Matching. Let A and B be two discrete images. Each image has M pixels. Let $H = (H_1, H_2, \ldots, H_L)$ be the histogram of A where H_l is the number of pixels in A with gray-level G_l. Let B^* denote the image B after histogram matching. If the pixel gray-levels in B are all distinct, then each pixel has a unique rank r_m associated with it. Then the histogram matching procedure is as follows.

$R_2 = 0$
`for` $l = 1 : L$
  $R_1 = R_2 + 1$; $R_2 = R_1 + H_l$;
  `for` $m = 1 : M$
    `if` $(R_1 \leq r_m \leq R_2)$; $B^*_m = G_l$; `end`
  `end`
`end`

[1] c^{-1} is defined as follows: If $y = c(x)$, then $c^{-1}(y) = x$.

6.2.1 Exact Histogram Specification

In many cases the number of pixels in an image, or an image patch, is much larger than the number of gray-levels. In this case, in order to obtain an exact histogram matching we require a method for ordering all the pixels which have the same gray-level. Traditionally, we order the pixels randomly. A better alternative is the following [2]. Separately convolve the image B with K small convolution masks $M_k, k \in \{1,2,\ldots,K\}$. Colute *et al.* [2] recommends the following six masks:

$$M_1 = \begin{pmatrix} 0&0&0&0&0\\ 0&0&0&0&0\\ 0&0&1&0&0\\ 0&0&0&0&0\\ 0&0&0&0&0 \end{pmatrix}, \quad M_2 = \begin{pmatrix} 0&0&0&0&0\\ 0&0&1&0&0\\ 0&1&1&1&0\\ 0&0&1&0&0\\ 0&0&0&0&0 \end{pmatrix}, \quad M_3 = \begin{pmatrix} 0&0&0&0&0\\ 0&1&1&1&0\\ 0&1&1&1&0\\ 0&1&1&1&0\\ 0&0&0&0&0 \end{pmatrix},$$

$$M_4 = \begin{pmatrix} 0&0&1&0&0\\ 0&1&1&1&0\\ 1&1&1&1&1\\ 0&1&1&1&0\\ 0&0&1&0&0 \end{pmatrix}, \quad M_5 = \begin{pmatrix} 0&1&1&1&0\\ 1&1&1&1&1\\ 1&1&1&1&1\\ 1&1&1&1&1\\ 0&1&1&1&0 \end{pmatrix}, \quad M_6 = \begin{pmatrix} 1&1&1&1&1\\ 1&1&1&1&1\\ 1&1&1&1&1\\ 1&1&1&1&1\\ 1&1&1&1&1 \end{pmatrix}.$$

Let $B_k(x,y), k \in \{1,2,\ldots,K\}$, denote the K outputs at the pixel (x,y), where by definition, $B_1(x,y) = B(x,y)$. We then order the pixels using the $B_k(x,y)$ as follows:

Example 6.3. Exact Histogram Specification [2].

```
for k = 1 : K
   If no ties exist, stop.
   Otherwise attempt to resolve ties using B_k.
end
If ties still exist resolve them randomly.
```

Once we have uniquely ordered the pixels according to b, i. e. each pixel has a unique integer rank $r(x,y)$ associated with it, we may then implement an exact histogram match as described in Ex. 6.2. *Note*. On the basis of r we may define a new image B', where

$$B'(x,y) = B(x,y) + \alpha r(x,y) ,$$

and α is a very small number [2]. By definition, the pixel gray-levels $B'(x,y)$ are unique but are still very close to the original gray-levels $B(x,y)$.

[2] If Δ denotes the smallest distance between adjacent gray-levels, then α should be less than Δ/N, where N is the number of pixels in the image.

Fig. 6.1 illustrates histogram equalization [3] using the exact histogram algorithm.

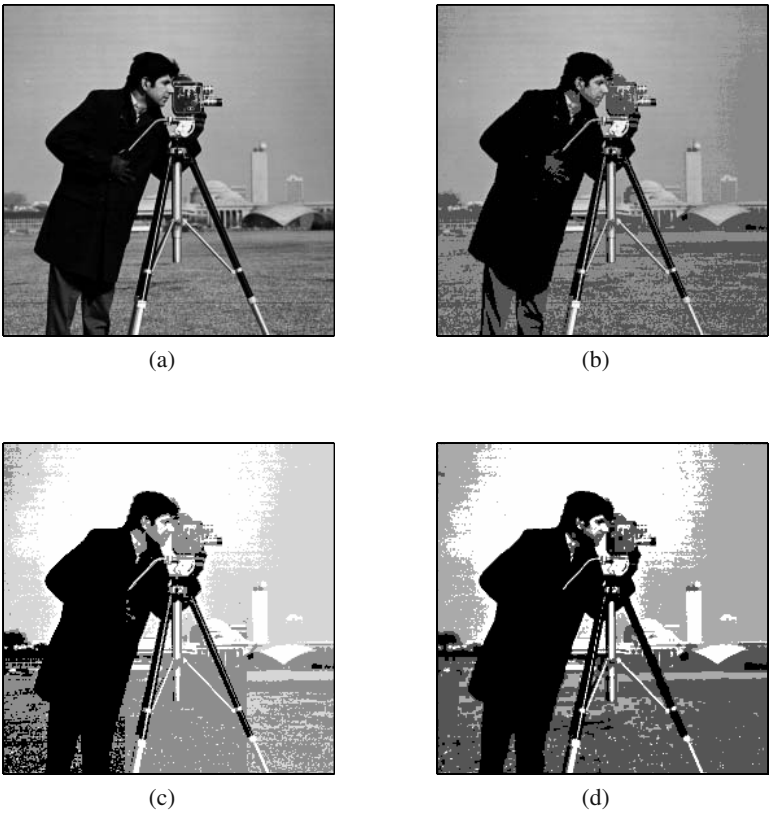

Fig. 6.1 **(a)** Shows an input image I with a full range of gray-levels. **(b)** Shows the result I_5 of histogram equalizing I to 5 levels. **(c)** Shows the result I'_4 of histogram equalizing I_5 to 4 levels using the traditional algorithm in which ties are randomly broken. **(d)** Shows the result I''_4 of histogram equalizing I_5 into 4 levels in which ties are broken using the exact histogram matching technique. We clearly see the improvement in image quality between I'_4 and I''_4.

6.3 Midway Image Equalization

Midway image equalization [3, 4] is defined as any method which warps two input histograms $p_A(a)$ and $p_B(b)$ to a common "intermediate" histogram p_Z, such that $p_Z(z)$ retains as much as possible of the shapes of $p_A(a)$ and $p_B(b)$. Mathematically,

[3] Histogram equalization is defined as a transformation of the gray-levels of an input image such that all gray-levels are equally populated.

[4] defines midway image equalization as follows: Given the two cumulative probability distributions $c_A(a)$ and $c_B(b)$ we define the intermediate distribution $p_Z(z)$ as the distribution whose inverse cumulative distance $c_Z^{-1}(z)$ is:

$$c_Z^{-1}(z) = \frac{c_A^{-1}(z) + c_B^{-1}(z)}{2} .$$

Suppose we warp $p_A(a)$ by matching it to $p_Z(z)$. Let $c_Z(z) = \int_0^z p_Z(z)dz$ denote the cumulative distribution of $p_Z(z)$, then the warped distribution is $p'_A(a')$, where

$$\begin{aligned} p'_A(a') &= p_A(a) , \\ a' &= c_Z^{-1}(c_A(a)) . \end{aligned}$$

Similarly we warp $p_B(b)$ by matching it to $p_Z(z)$. The corresponding warped distribution is $p'_B(b')$, where

$$\begin{aligned} p'_B(b') &= p_Z(b) , \\ b' &= c_Z^{-1}(c_B(b)) . \end{aligned}$$

The midway image equalization procedure may be implemented in an efficient manner using a dynamic programming technique [3]. However, when the images are of the same size and pixel gray-levels in each image are unique (i. e. no two pixels have the same gray-level) [4] we may implement a midway image equalization scheme as explained in the following example.

Example 6.4. Simple Midway Image Equalization. Given two $M \times N$ input images A and B in which all pixels have a unique gray-level, let $a_{(i)}$ and $b_{(i)}$ denote, respectively, the ith smallest gray-level in A and B. Then the corresponding midway gray-level is c_i, where

$$c_i = (a_{(i)} + b_{(i)})/2 .$$

Pseudo-code for calculating the midway equalized images A' and B' is:

$[As, invrA] = sort(A(:)); [junk, rA] = sort(invrA);$
$[Bs, invrB] = sort(B(:)); [junk, rB] = sort(invrB);$
$C = (As + Bs)/2;$
`for` $i = 1 : M * N$
    $h = rA(i); A'(i) = C(h); k = rB(i); B'(i) = C(k);$
`end`
$A' = reshape(A', M, N); B' = reshape(B', M, N);$

[4] If the pixels in the images are not unique then we may use the exact histogram specification scheme (Sect. 6.2.1) to create images whose gray-levels are unique.

6.4 Matching Second-Order Statistics

A simple version of histogram matching is to match the second-order statistics of the input images. Given two input images A and B of the same scene, we map the gray-levels of B so that the mean and standard deviation of B matches that of A. Let μ_A and μ_B denote the mean gray-level of A and B and let σ_A and σ_B denote the standard deviation of A and B. If $\widetilde{B}(m,n)$ denotes the gray-level of B after scaling, then

$$\widetilde{B}(m,n) = (B(m,n) - \mu_B)\frac{\sigma_A}{\sigma_B} + \mu_A \ .$$

Although very simple, matching second-order statistics is still widely used in remote sensing applications. In fact, in some applications [7], it may be preferred over histogram matching. For example, in merging infra-red and visible light images, Li and Wang [7] found it is preferable to perform radiometric calibration by matching the second-order statistics of the two images.

6.5 Ranking

Ranking is a robust method for radiometric normalization which like histogram matching does not require any training data. The following example illustrates the concept of ranking in remote sensing.

Example 6.5. Remote Sensing [8]. Remotely sensed data are increasingly used for mapping and monitoring the physical environment. One of the advantages of monitoring with remotely sensed data is that temporal sequences can accurately indicate environmental changes, assuming that the input data is radiometrically consistent for all scenes. Factors contributing to the potential inconsistency in measured radiance include changes in surface condition, illumination geometry, sensor calibration, observation geometry and atmospheric condition. By using a radiometric normalization technique, we may however, correct for data inconsistencies resulting from many different effects. Image normalization is carried out in one step by converting image values to ordinal ranks. Ordinal ranking allows us to assign each pixel a new value based on its reflectance value, relative to all other pixels. When image pairs are converted to ordinal ranks the global characteristics of the distributions of pixel values are matched.

Pixel ranking does not require atmospheric details, sensor information, or selection of subjective pseudo-invariant features, and therefore allows images to be simply and efficiently normalized and processed for changes with minimal *a priori* knowledge. In general, for small pictures, pixel ranking is an effective image normalization technique. It is less effective on very large digital images because in this case we obtain many tied ranks, although the exact ordering technique discussed in Sect. 6.2.1 may help.

6.6 Thresholding

In image thresholding we convert an input image I into a binary labeled image B using a threshold gray-level t:

$$B(x,y) = \begin{cases} 1 \text{ if } I(x,y) \geq t \ , \\ 0 \text{ otherwise} \ . \end{cases} \tag{6.1}$$

The primary purpose of a thresholding algorithm is to segment the input image into background regions and foreground regions or objects of interest. However, image thresholding is sometimes also used as a simple method for radiometric normalization. The following algorithm describes the Otsu thresholding algorithm.

Example 6.6. Otsu thresholding algorithm [9]. Given an input picture I, let $g(x,y)$ denote the gray-level at pixel (x,y). Then pixel gray-levels are divided into two groups: foreground pixels whose gray-levels are less than, or equal to, a threshold t and background pixels whose gray-levels are greater than t. The optimum threshold is found by maximizing the separation between the two groups. Let $\mu_F(t)$, $\sigma_F(t)$ and $\mu_B(t)$, $\sigma_B(t)$ denote, respectively, the mean gray-level and standard deviation of the foreground and background pixels (defined with a threshold t), then the optimum threshold is given by

$$t_{OPT} = \arg\max_t \left(\frac{P(t)\,(1-P(t))\,(\mu_F(t)-\mu_B(t))^2}{P(t)\sigma_F^2(t)+(1-P(t))\,\sigma_B^2(t)} \right) ,$$

where $P(t)$ is the relative number of pixels with gray-level less than, or equal to, t.

In some applications the conversion of the pixel gray-levels $I(x,y)$ in the input image into binary gray-levels $B(x,y)$ using (6.1) is too coarse. In these cases, we may use a fuzzy thresholding algorithm which generates a fuzzy gray-level image $\widetilde{B}$, where $\widetilde{B}(x,y) \in [0,1]$.

Fig. 6.2 shows the result of thresholding an input image.

The following example illustrates the use of local thresholding for radiometric calibration.

Example 6.7. Local Binary Pattern for Radiometric Calibration [5, 6]. Ref. [5, 6] describes the use of the local binary pattern (LBP) operator as an efficient method for radiometric calibration of face images in an *uncontrolled* environment. The LBP operator (see Sect. 3.4) works as follows. It takes a local neighborhood around each pixel and thresholds the pixels in the neighborhood according to the value of the center pixel. The weighted sum of the thresholded pixels is a label which may be regarded as a radiometrically calibrated pixel value (see Fig. 3.5). For a 3×3 neighborhood centered on the

(a) (b)

Fig. 6.2 **(a)** Shows an input image I. **(b)** Shows the binary image after thresholding I with the Otsu algorithm.

pixel (m,n), the LBP operator is defined as

$$LBP(m,n) = \sum_{k=0}^{7} s(A(m,n),A(i_k,j_k))2^{(k-1)} ,$$

where (i_k,j_k) are the coordinates of the kth pixel in the 3×3 neighborhood of (m,n) and

$$s(A(m,n),A(i_k,j_k)) = \begin{cases} 1 \text{ if } A(i_k,j_k) > A(m,n) , \\ 0 \text{ otherwise} . \end{cases}$$

Note: The operator may be extended to circular neighborhoods by bilinearly interpolating the pixel values [6].

6.7 Segmentation

In image segmentation we convert an input image into a multiple label image. Although segmentation is primarily a diagnostic tool in which the input image is decomposed into contiguous regions, we may also use it as a method for radiometric normalization. The following example illustrates a simple K-means cluster algorithm which may be used for image segmentation.

Example 6.8. K-means cluster algorithm. Given an input image I with pixel gray-levels $g_m, m \in \{1,2,\ldots,M\}$. Let $G_1,G_2,\ldots,G_K$ denote K cluster centers or cluster gray-levels. Each pixel gray-level g_m is associated with a given cluster:

$$\delta_{mk} = \begin{cases} 1 \text{ if } g_m \text{ is associated with } G_k \,, \\ 0 \text{ otherwise} \,. \end{cases}$$

Then the K-means algorithm attempts to find the set of cluster centers $G_k, k \in \{1,2,\ldots,K\}$, such that the total error is a minimum:

$$(G_1, G_2, \ldots, G_K) = \arg\min_{G_k} \sum_{m=1}^{M} \sum_{k=1}^{K} \delta_{mk} C(g_m, G_k) \,,$$

where C is an appropriate cost function. A common cost function is $C(x,y) = |x-y|$.

The K-means algorithm works in an iterative manner as follows: In each iteration we calculate the assignment matrix δ_{mk} using the cluster centers G_k calculated in the previous iteration. The cluster centers are then recalculated using the new assignment matrix. The process for T iterations is:

```
for t = 1 : T
    for m = 1 : M
      δ_mk^(t) = { 1 if |g_m − G_k^(t−1)| = min_l |g_m − G_l^(t−1)|;
                 { 0 otherwise;
    end
    for k = 1 : K
      G_k^(t) = Σ_{m=1}^{M} δ_mk^(t) g_m / Σ_{m=1}^{M} δ_mk^(t) ;
    end
end
```

Fig. 6.3 illustrates the segmentation of an input image using the K-means cluster algorithm. Although very simple the K-means cluster algorithm is widely used as a method of image segmentation. Recently with the development of ensemble learning, the K-means algorithm is found to be capable of giving state-of-the-art segmentation (see Chapt. 16).

Note: Although image segmentation is an effective method for radiometric calibration, the segmented images may still require semantic equalization (see Sect. 5.3).

6.8 Feature Map Normalization

Although in many cases, feature map normalization requires the maps to be brought into semantic equivalence, there are cases when the feature maps measure the same object, or phenomena, and semantic equivalence is not required. In this case, the feature maps may be normalized using any of the techniques discussed previously.

(a) (b)

Fig. 6.3 **(a)** Shows an input image I. **(b)** Show the segmentation of I using the K-means algorithm with $K = 6$.

Example 6.9. Multiple Edge Maps. We consider an input image on which we apply a Sobel and a Canny edge detectors. The two detectors work on different principles but both measure the presence, or otherwise, of an edge in the input image. The two feature maps, F_{sobel} and F_{canny}, are clearly semantically equivalent. They may therefore be fused together if the feature maps F_{sobel} and F_{canny} are radiometrically aligned to the same scale. If we use a simple linear radiometric scale, the corresponding calibrated maps are:

$$\lambda_{sobel}(x,y) = \frac{F_{sobel}(x,y) - F^{\min}_{sobel}}{F^{\max}_{sobel} - F^{\min}_{sobel}},$$

$$\lambda_{canny}(x,y) = \frac{F_{canny}(x,y) - F^{\min}_{canny}}{F^{\max}_{canny} - F^{\min}_{canny}},$$

where $F^{\min}_{sobel} = \min_{(x,y)} F_{sobel}(x,y)$, $F^{\max}_{sobel} = \max_{(x,y)} F_{sobel}(x,y)$, $F^{\min}_{canny} = \min_{(x,y)} F_{canny}(x,y)$ and $F^{\max}_{canny} = \max_{(x,y)} F_{canny}(x,y)$.

6.9 Probabilistic Scale

In Ex. 5.2 we described making two feature maps semantically equivalent by converting them into probabilistic, or likelihood, maps. This transformation may also be used for radiometric calibration.

6.10 Software

GPAV. A matlab toolbox for isotonic regression. Authors: Oleg Burdakov, Anders Grimvall and Oleg Sysoev [1].

LIBRA. A toolbox for performing classical and robust statistics. The toolbox contains m-files on various robust normalization techniques. Authors: Sabine Verboven and Mia Hubert [11].

MATLAB STATISTICAL TOOLBOX. Matlab statistical toolbox. The toolbox contains m-files for performing various radiometric calibration procedures.

STPRTOOL. A statistical pattern recognition toolbox. Authors: Vojtech Franc and Vaclav Hlovac. The toolbox contains a file mlsigmoid.m which performs Platt calibration.

6.11 Further Reading

In this chapter we have given a brief overview of some relative calibration methods which have general applicability. However, for specific applications, specialized normalization techniques may be available. For example, [10] contains a comparison of different radiometric calibration algorithms for face verification.

References

1. Burdakov, O., Grimvall, A., Sysoev, O.: Data preordering in generalized PAV algorithm for monotonic regression. J. Comp. Math. 24, 771–790 (2006)
2. Coltue, D., Bolon, P., Chassery, J.-M.: Exact histogram specification. IEEE Trans. Image Process. 15, 1143–1152 (2006)
3. Cox, I., Roy, S., Hingorani, S.L.: Dynamic histogram warping of image pairs for constant image brightness. In: Proc. IEEE Int. Conf. Image Process., vol. 2, pp. 366–369 (1995)
4. Delon, J.: Midway image equalization. J. Math. Imag. Vis. 21, 119–134 (2004)
5. Heusch, G., Rodriguez, Y., Marcel, S.: Local binary patterns as an image pre-processing for face authentification. In: Proc. FGR (2006)
6. Holappa, J., Ahonen, T., Pietikainen, M.: An optimized illumination normalized method for face recognition. In: Second IEEE Int. Conf. Biometrics: Theory Appl. Systems (2008)
7. Li, G., Wang, K.: Merging infrared and color visible images with a contrast enhanced fusion method. In: Proc. SPIE, vol. 6571, p. 657108 (2007)
8. Nelson, T., Wilson, H.G., Boots, B., Wulder, M.A.: Use of ordinal conversion for radiometric normalization and change detection. Int. J. Remote Sensing 26, 535–541 (2005)
9. Otsu, N.: A threshold selection method from gray-level histogram. IEEE Trans. Syst. Man Cybernetics 9, 62–66 (1979)
10. Short, J., Kittler, J., Messer, K.: A comparison of photometric normalization algorithms for face authentification. In: Proc. AFGR (2004)
11. Verboven, S., Hubert, M.: Libra: A matlab library for robust analysis. Chemometrics and Intell. Laboratory Syst. 75, 127–136 (2005)
12. Zhuge, Y., Udupa, J.K.: Intensity standardization simplifies brain MR image segmentation. Comp. Vis. Image Under. 113, 1095–1103 (2009)